

Quantitative Acetylomics Reveals Dynamics of Protein Lysine Acetylation in Mouse Livers During Aging and Upon the Treatment of Nicotinamide Mononucleotide

Authors

Jingshu Li, Ye Cao, Kongyan Niu, Jiaqian Qiu, Han Wang, Yingnan You, Dean Li, Yu Luo, Zhengjiang Zhu, Yaoyang Zhang, and Nan Liu

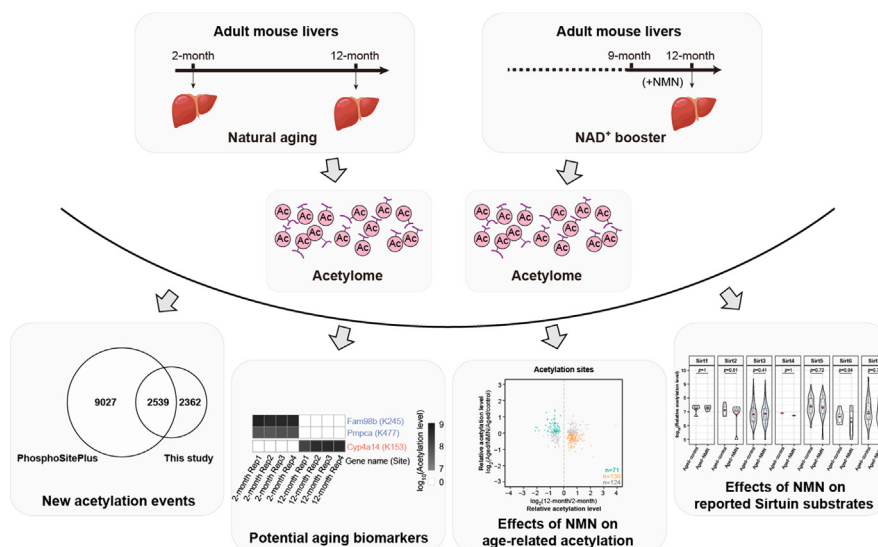
Correspondence

zyy@sioc.ac.cn; liunan@sioc.ac.cn

Graphical Abstract

In Brief




Li *et al.* have performed label-free quantification of the acetylomes in mouse livers with age and upon the treatment of nicotinamide mononucleotide (NMN), revealing previously unknown acetylation events. The datasets characterize not just the dynamics of acetylation with age but also specific acetylation sites as new aging biomarkers. The investigation indicates that the life-beneficial effect of NMN could be partially reflected by the changes in age-related protein acetylation. NMN has mild effects on acetylation previously reported as substrates of Sirtuins.



Highlights

- Acetylomes from mouse livers are studied with age and NMN treatment.
- Protein acetylation events are discovered as potential aging biomarkers.
- Life-beneficial effect of NMN could be partly reflected by acetylation changes.
- NMN has mild effects on acetylation sites reported as substrates of Sirtuins.

Quantitative Acetylomics Reveals Dynamics of Protein Lysine Acetylation in Mouse Livers During Aging and Upon the Treatment of Nicotinamide Mononucleotide

Jingshu Li^{1,2,‡}, Ye Cao^{1,2,‡}, Kongyan Niu^{1,2}, Jiaqian Qiu^{1,2}, Han Wang^{1,2}, Yingnan You^{1,2}, Dean Li^{1,2}, Yu Luo³, Zhengjiang Zhu¹, Yaoyang Zhang^{1,*}, and Nan Liu^{1,*}

Lysine acetylation is a reversible and dynamic post-translational modification that plays vital roles in regulating multiple cellular processes including aging. However, acetylome-wide analysis in the aging process remains poorly studied in mammalian tissues. Nicotinamide adenine dinucleotide (NAD⁺), a hub metabolite, benefits health span at least in part due to the activation of Sirtuins, a family of NAD⁺-consuming deacetylases, indicating changes in acetylome. Here, we combine two antibodies for the enrichment of acetylated peptides and perform label-free quantitative acetylomic analysis of mouse livers during natural aging and upon the treatment of beta-nicotinamide mononucleotide (NMN), a NAD⁺ booster. Our study describes previously unknown acetylation sites and reveals the acetylome-wide dynamics with age as well as upon the treatment of NMN. We discover protein acetylation events as potential aging biomarkers. We demonstrate that the life-beneficial effect of NMN could be partially reflected by the changes in age-related protein acetylation. Our quantitative assessment indicates that NMN has mild effects on acetylation sites previously reported as substrates of Sirtuins. Collectively, our data analyze protein acetylation with age, laying critical foundation for the functional study of protein post-translational modification essential for healthy aging and perhaps disease conditions.

Protein acetylation is one of the vital protein post-translational modifications (PTMs) that have been shown to impact various cellular processes, including DNA-histone compactness (1), activity of enzymes (2), protein aggregation (3), and protein stability (4). Protein acetylation occurs irreversibly on the α -amino group at the N-terminal amino acid (5) or reversibly on the ϵ -amino group on the side chain of the lysine residue. Since lysine acetylation is a reversible and thus

dynamic process, proteome-wide quantitative characterization of lysine acetylation, the acetylome, is crucial to understand the regulatory role of acetylation. Though proteomic survey of acetylation has been reported in cell lines (6–8) and organisms, such as fly (9), mouse (10), rat (11), and human (4), dynamics of acetylome during aging process remains poorly described.

Aging is characterized by a progressive loss of physiological integrity, leading to impaired function and increased vulnerability to death (12). Accumulating evidence has indicated critical roles of protein acetylation in aging. For instance, acetylation of Microtubule-associated protein tau (Tau) at K280 has been linked with normal brain aging as well as a wide spectrum of human neurodegenerative diseases including Alzheimer's disease (13, 14), suggesting the potential of lysine acetylation as aging biomarkers. A small-scale acetylome study in the fly head reveals an increase in 79 and a decrease in 3 acetylation sites from 217 high-confidence acetylation events in midlife flies than in those of young flies (9). In mouse hind limb and cardiac muscles, Western blot experiments show that the bulk level of muscle protein acetylation is significantly increased in aged animals (15). However, aging acetylome analysis in mammalian tissues with a resolution at single peptides remains to be addressed.

Nicotinamide adenine dinucleotide (NAD⁺) is a hub metabolite involving in a wide range of cellular processes (16). NAD⁺ has been reported to decline with age in mammalian organs (17–19). Boosting NAD⁺ biosynthesis, by supplementation of precursors such as beta-nicotinamide mononucleotide (NMN), triggers life span extension of yeasts (20), worms (21), flies (22), and mice (23), ameliorating age-related diseases (17, 24, 25). Studies have demonstrated that such beneficial effects of NAD⁺ are at least in part due to the

From the ¹Interdisciplinary Research Center on Biology and Chemistry, Shanghai Institute of Organic Chemistry, Chinese Academy of Sciences, Shanghai, China; ²University of Chinese Academy of Sciences, Beijing, China; ³Abiochem Biotechnology, Shanghai, China

[‡]These authors contributed equally to this work.

*For correspondence: Nan Liu, liunan@sioc.ac.cn; Yaoyang Zhang, zyy@sioc.ac.cn.

activation of Sirtuins (20–22, 26–28), a family of NAD⁺-consuming deacetylases (29), indicating changes in acetylation. However, the extent of NAD⁺-induced dynamics in protein acetylation remains unknown. Here, using a dual-antibody enrichment protocol combined with high-resolution liquid chromatography with tandem mass spectrometry (LC-MS/MS) analysis, we performed the label-free quantification of the acetylomics in mouse livers with age and upon the treatment of NMN, revealing previously unknown acetylation events. Our dataset characterized not just the dynamics of acetylation with age but also specific acetylation sites as new aging biomarkers. We further investigated the impact of NMN treatment on protein acetylation.

EXPERIMENTAL PROCEDURES

Ethics Statement

All animal procedures have been reviewed and approved by the Institutional Animal Care and Use Committee at the Chinese Academy of Sciences (202003180013) and were in accordance with the Guide for the Care and Use of Laboratory Animals of the Chinese Academy of Sciences. All efforts were made to minimize the suffering of the animals.

Animal Experimentation

C57BL/6 male mice were housed in an environmentally controlled room under a 12:12-h light/dark cycle at 23 °C and were fed with commercial mouse chow food and water ad libitum. For treatment of beta-nicotinamide mononucleotide (NMN), 9-month-old C57BL/6 mice were supplemented with NMN (Abiochem) dissolved in sterile water (500 mg/kg/d) for 3 months until 12 months of age. NMN water was changed every other day. Four mice were used in 2-month, 12-month and Aged-control experiments, and three mice were used in Aged-NMN experiments. Livers were dissected and immediately frozen in liquid nitrogen.

Sample Preparation for LC-MS/MS

Mouse liver tissues were homogenized in ice-cold urea lysis buffer containing 8 M urea, 100 mM Tris-hydrochloride (Tris-HCl), pH 8.5, 150 mM sodium chloride (NaCl), and protease inhibitor (Roche). Cell lysates were incubated on ice for 20 min before addition of 1/10 volume 5 M NaCl to release chromatin-bound proteins. The lysates were sonicated to shear genomic DNA and were clarified by centrifugation at 14,000 rcf for 15 min at 4 °C. The protein concentration of the supernatant was determined by the bicinchoninic acid protein assay (Thermo Fisher Scientific). Samples containing 2 mg of proteins were reduced with 5 mM tris(2-carboxyethyl)phosphine (20 min at room temperature), alkylated with 10 mM iodoacetamide (15 min at room temperature in the dark), diluted by a factor of 4 with 100 mM Tris-HCl, pH 8.5 (final concentration of urea was equal to 2 M), and incubated overnight at 37 °C with sequencing-grade trypsin (Promega) added at a 1:100 enzyme:substrate ratio (wt/wt). Samples were then acidified with formic acid (FA) and desalted using solid-phase extraction cartridges C18. Ten micrograms of peptides of each sample was collected as input. The remaining samples were immunoprecipitated with 20 µl of acetyl lysine antibody, agarose (1:1) (ICP0388, ImmuneChem; PTM-104, PTM Biolabs). Agarose was washed by wash buffer I (100 mM NaCl, 1 mM ethylenediaminetetraacetic acid [EDTA], 20 mM Tris-HCl, 0.5% Nonidet P-40; adjust pH to 8.0), wash buffer II (100 mM NaCl, 1 mM EDTA, 20 mM Tris-HCl; adjust pH to 8.0), and

ddH₂O. Finally, the acetylated peptides were eluted with 0.1% trifluoroacetic acid (TFA).

LC-MS/MS for Proteome and Acetylome

The input peptides and enriched acetylated peptides were analyzed by an online LC-MS system that consisted of an Easy-nLC-1200 HPLC (Thermo Fisher Scientific) and a Q Exactive HF-X mass spectrometer (Thermo Fisher Scientific). Peptides were loaded directly onto a 300-mm-long analytical column (100 µm I.D., 1.9 µm C18 resin) housed in a column oven at 60 °C. A 240-min gradient (3% B at 0 min, 10% B at 2 min, 20% B at 177 min, 40% B at 217 min, 50% B at 224 min, 100% B at 225 and 240 min) (A: 0.1% FA in water, B: 0.1% FA, and 80% acetonitrile [ACN] in water) was developed to separate the peptides at a static flow rate of 300 nl/min. For MS1, the scan range of MS was 350 to 1500 m/z at a resolution of 60,000 and the AGC target was 5e6. The maximum injection time for the precursor ion was 20 ms. Top 10 precursor ions with charge states from 2+ to 6+ were selected for fragmentation. Dynamic exclusion was enabled for 0.5 min. High-energy collisional dissociation was used to fragment the precursor peptides with a normalized collision energy of 27. The resolution of MS2 was set to 60,000, while the AGC target was set to 2e5 with a maximum injection time of 20 ms for input peptides and 120 ms for enriched acetylated peptides.

Peptide Identification and Quantification

MS data were analyzed by MaxQuant (version 1.6.0.1) (30) and were searched against the SwissProt mouse protein database (released in Jun 2017). The precursor and fragment mass tolerances were 20 ppm. Trypsin was set as the enzyme, and the maximum missed cleavage was set to 2. The carbamidomethylation (+57.0125 Da) of cysteine was set as a static modification. The acetylation (+42.0106 Da) of lysine and protein N-terminal and the oxidation (+15.9959 Da) of methionine were defined as variable modifications. The false discovery rate at peptide spectrum match level was controlled below 1% using a target-decoy approach. “Match between runs” was used during data analysis, and the match time window was set within 0.7 min.

Input (Proteomic) data of mouse livers (2 months and 12 months) were searched together since they were processed in one batch. Input data of NMN-treated and age-matched control mouse livers (Aged-NMN and Aged-control) were analyzed in a separate search. The intensities for protein levels were first divided by the ratio of the sum intensity of each replicate in every group. Then, missing values were labeled as “NA” and the average levels were calculated using intensities in the remaining replicates. Proteins with more than two missing values in each group were filtered out. The ratios of average protein levels of 2 months:12 months and the ratios of average protein levels of Aged-control:Aged-NMN were calculated for normalization of the acetylomic data.

Enrichment (Acetylomic) data of mouse livers (2 months and 12 months) were searched together, and enrichment data of NMN-treated and age-matched control mouse livers (Aged-NMN and Aged-control) were analyzed in another search. The intensities for acetylation levels were first divided by the ratio of the sum intensity of each replicate in every group. Then, missing values were served as “NA” and the average levels were calculated using intensities in the remaining replicates. Acetylation sites with more than two missing values in each group were filtered out. Acetylation sites whose corresponding protein abundances were not quantified were also filtered out. The relative acetylation levels were the acetylation levels divided by the protein ratio of 12-months/2-months or Aged-NMN/Aged-control.

LC-MS for the Detection of Nicotinamide Adenine Dinucleotide, Oxidized Form (NAD⁺)

Mouse liver tissues were homogenized with 200 μ l of H₂O and 20 ceramic beads (0.1 mm) using the homogenizer (Bertin Technologies, France). Eight hundred microliters of methanol (MeOH):ACN (1:1, v/v) was added for metabolite extraction. To precipitate the protein, samples were incubated for 1 h at -20°C , followed by 15 min of centrifugation using 14,000 rcf at 4°C . The supernatants were removed and evaporated to dryness in a vacuum concentrator (Lab-conco). Dry extracts were then reconstituted in 100 μ l of ACN:H₂O (1:1, v/v), followed by 10 min of sonication (50 Hz, 4°C) and 15 min of centrifugation using 14,000 rcf at 4°C to remove insoluble debris. Supernatants were transferred to HPLC glass vials and stored at -80°C prior to LC-MS analysis.

The LC-MS analysis was performed using a UHPLC system (1290 series, Agilent Technologies) coupled to a triple quadrupole mass spectrometer (Agilent QqQ 6495, Agilent Technologies). A Waters ACQUITY UPLC BEH Amide column (100 \times 2.1 mm; particle size, 1.7 μ m; 130 \AA , Waters) was used for separation, and the column temperature was kept at 25°C . The mobile phase A was 25 mM ammonium hydroxide (NH₄OH) and 25 mM ammonium acetate (NH₄OAc) in water, and B was ACN. The linear gradient was set as follows: 0 to 0.5 min: 95% B, 0.5 to 7 min: 95% B to 65% B, 7 to 8 min: 65% B to 40% B, 8 to 9 min: 40% B, 9 to 9.1 min: 40% B to 95% B, and 9.1 to 12 min: 95% B. The flow rate was 0.5 ml/min, and the sample injection volume was 2 μ l. The measurement was performed in positive and negative modes. ESI source parameters were set as follows: sheath gas temperature, 350°C ; dry gas temperature, 170°C ; sheath gas flow, 12 L/min; dry gas flow, 16 L/min; capillary voltage, 3000 V or -2500 V in positive or negative modes, respectively; nozzle voltage, 1000 V and -1500 V in positive and negative modes, respectively; and nebulizer pressure, 40 psi. For the analyses of NAD⁺, several MRM transitions were simultaneously monitored, including 664.1/136.3 for quantification and 664.1/428.0 and 664.1/231.8 for qualification. The dwell time for each MRM transition was 50 ms. The MRM transitions were obtained using the purchased chemical standard of NAD⁺ (10 μ g/ml) and optimized using the MassHunter Optimizer software (version B.07.01, Agilent Technologies). The peak areas of quantification transition (*i.e.*, 664.1/136.3) were manually integrated for relative quantitative analysis using the Agilent Qualitative software (version B.07.00, Agilent Technologies).

Bioinformatic Analysis

Gene Ontology (GO) and Kyoto Encyclopedia of Genes and Genomes (KEGG) pathway analysis were performed by the Database for Annotation, Visualization and Integrated Discovery (DAVID) (version 6.8) (31, 32). Bar plots were generated by GraphPad Prism (version 8.3.0, GraphPad). Venn diagrams were plotted by R package eulerr (version 6.1.1). Correlation matrixes were performed with the ggpairs function of the R package GGally (version 2.1.2). The UpSet plot was generated by R package upSetR (version 1.4.0). Pie chart, scatterplot, and violin plot were produced by R package ggplot2 (version 3.3.5). Heatmaps were plotted by R package pheatmap (version 1.0.12).

RESULTS

Acetylome Studies Reveal Previously Uncharacterized Protein Acetylation in Mouse Livers

To profile protein acetylation with age, we performed proteome-wide acetylation studies. We examined adult mouse at young (2 months) and aged condition (12 months). In addition, we supplemented NMN to a 9-month-old mouse for

3 months to result in 12 months of age (Aged-control versus Aged-NMN). To enhance the broadness of epitope coverage for immunoprecipitation, we combined two antibodies for the enrichment of acetylated peptides (Fig. 1A). From mouse liver tissues, this strategy led us to identify 4,146, 4,088, 3,251, and 3121 acetylation sites from 2-month-old (four biological replicates), 12-month-old (four biological replicates), Aged-control (four biological replicates), and Aged-NMN (three biological replicates) mice, respectively (supplemental Table S1). Among them, 3,798, 3,915, 2,991, and 2797 acetylation sites were reproducibly identified from at least two out of the biological replicates (supplemental Fig. S1A and supplemental Table S1). Comparison of the biological replicates revealed a correlation coefficient equal to or higher than 0.919, indicating high reproducibility (supplemental Fig. S1B). Nearly half of acetylated proteins (45.10%, 45.98%, 49.24%, and 49.41% from 2-month-old, 12-month-old, Aged-control, and Aged-NMN mice, respectively) contained one acetylation site, while more than half proteins (54.90%, 54.02%, 50.76%, and 50.59%) had more than one acetylation sites, and notably, a small proportion of proteins (4.71%, 2.07%, 4.56%, and 4.55%) were found to have equal or even higher than 10 acetylation sites (Fig. 1B).

PhosphoSitePlus comprises 11,564 nonredundant acetylation sites from the mouse (33). Comparative analysis indicated not just 2539 common acetylation sites but also 2362 potentially new acetylation sites as revealed by the current study (Fig. 2A and supplemental Table S2), adding new information to the PhosphoSitePlus repertoire. GO on our acetylome data found that acetylated proteins in mouse livers were mainly involved in the oxidation–reduction process, translation, and metabolism (Fig. 2B and supplemental Table S2). Molecular functions of the acetylated proteins were primarily in poly(A) RNA binding, oxidoreductase activity, and catalytic activity (Fig. 2B and supplemental Table S2). The acetylated proteins were localized in mitochondrion, intracellular ribonucleoprotein complex, and cytosol (Fig. 2B and supplemental Table S2). KEGG pathway analysis revealed the enrichment of metabolism pathways, biosynthesis of antibiotics, and carbon metabolism (Fig. 2B and supplemental Table S2).

Age-Associated Dynamics in Protein Acetylation

We compared the dynamics of acetylation sites between young and aged animals. To diminish the alternations of protein basal levels that naturally occur with age, changes in acetylation were normalized to the expression of their host protein. Our analysis showed that 155 acetylation sites from 139 proteins were unique in 2-month-old mouse livers (supplemental Fig. S2A and supplemental Table S3), with their functions mainly involved in fatty acid beta-oxidation, oxidation–reduction process, translation, acetyl-CoA metabolism, and oxaloacetate metabolism (Fig. 3A and supplemental Table S3). On the other hand, 156 acetylation

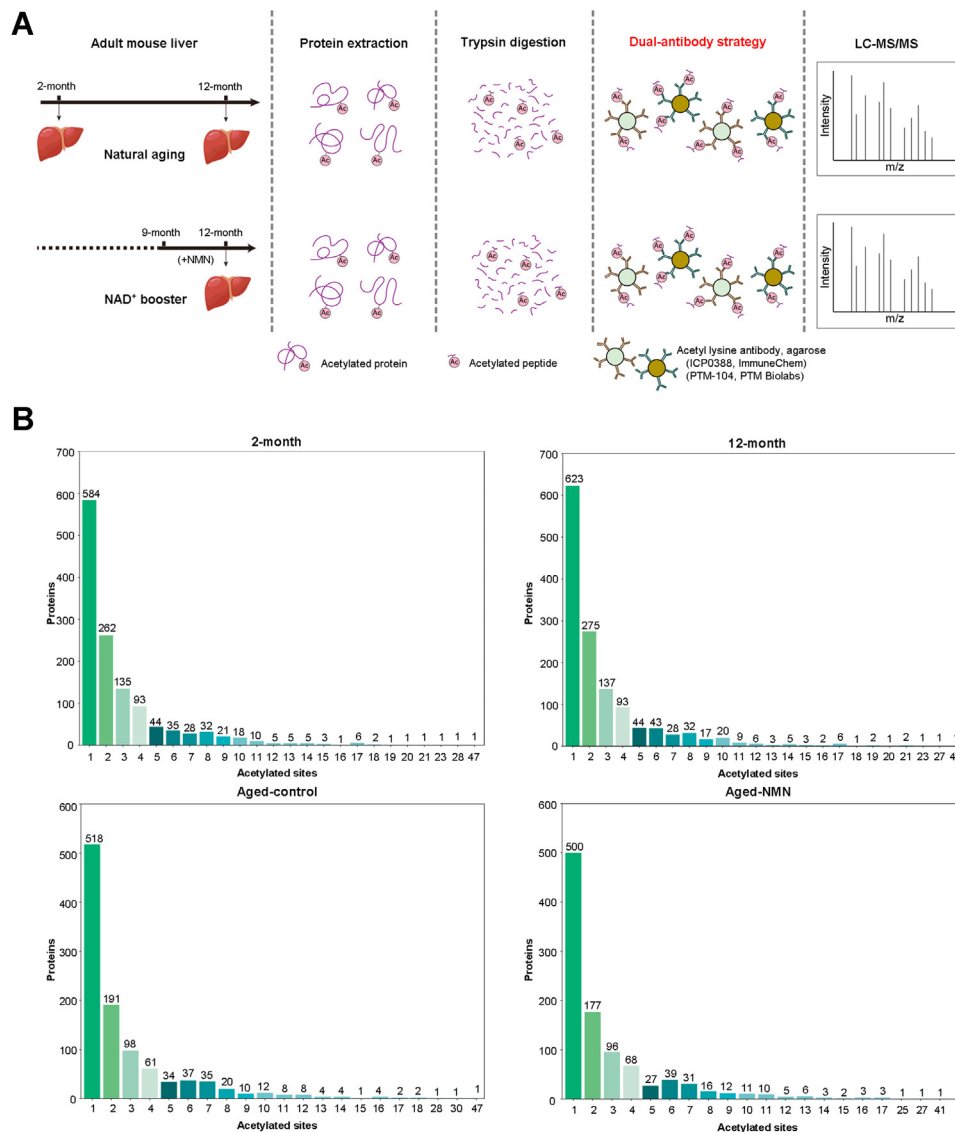


FIG. 1. **Global assessment of acetylome in adult mouse livers.** A, scheme for dual-antibody-based acetylome profiling from adult mouse livers during natural aging and upon the treatment of NAD⁺ booster. B, distribution number of the acetylation sites per protein.

sites from 131 proteins were only identified in 12-month-old mouse livers (supplemental Fig. S2A and supplemental Table S3). GO analysis revealed their roles in fatty acid beta-oxidation, oxidation-reduction process, translation, biosynthesis, and valine catabolism (Fig. 3A and supplemental Table S3). Among 3370 acetylation sites found in both young and aged animals (supplemental Fig. S2A and supplemental Table S3), 137 sites from 111 proteins were significantly decreased with age (2-months/12-months > 1.5, $p < 0.05$), while 288 sites from 218 proteins were increased (12-months/2-months > 1.5, $p < 0.05$) (Fig. 3B and supplemental Table S3). Proteins that had decreased acetylation with age were enriched in oxidation-reduction process, protein folding, protein homotetramerization, fatty acid beta-oxidation, tricarboxylic acid cycle, response to drug, cell redox homeostasis,

and arginine biosynthesis (Fig. 3C and supplemental Table S3), while acetylation events that had late-onset increase were mainly involved in oxidation-reduction process, translation, protein folding, protein homotetramerization, metabolic processes of fatty acid, triglyceride, and glycine (Fig. 3C and supplemental Table S3). During aging, acetylation events involved in the oxidation-reduction process were notably enriched (Fig. 3, A and C). Detailed characterization determined that acetylation of the redox proteins in tricarboxylic acid cycle was upregulated with age except for Malate dehydrogenase, mitochondrial (Fig. 3D and supplemental Table S3). Apart from K227 on Alcohol dehydrogenase 1, protein acetylation in retinol metabolism increased with age (Fig. 3D and supplemental Table S3). Proteins in arachidonic acid metabolism and steroid biosynthesis demonstrated

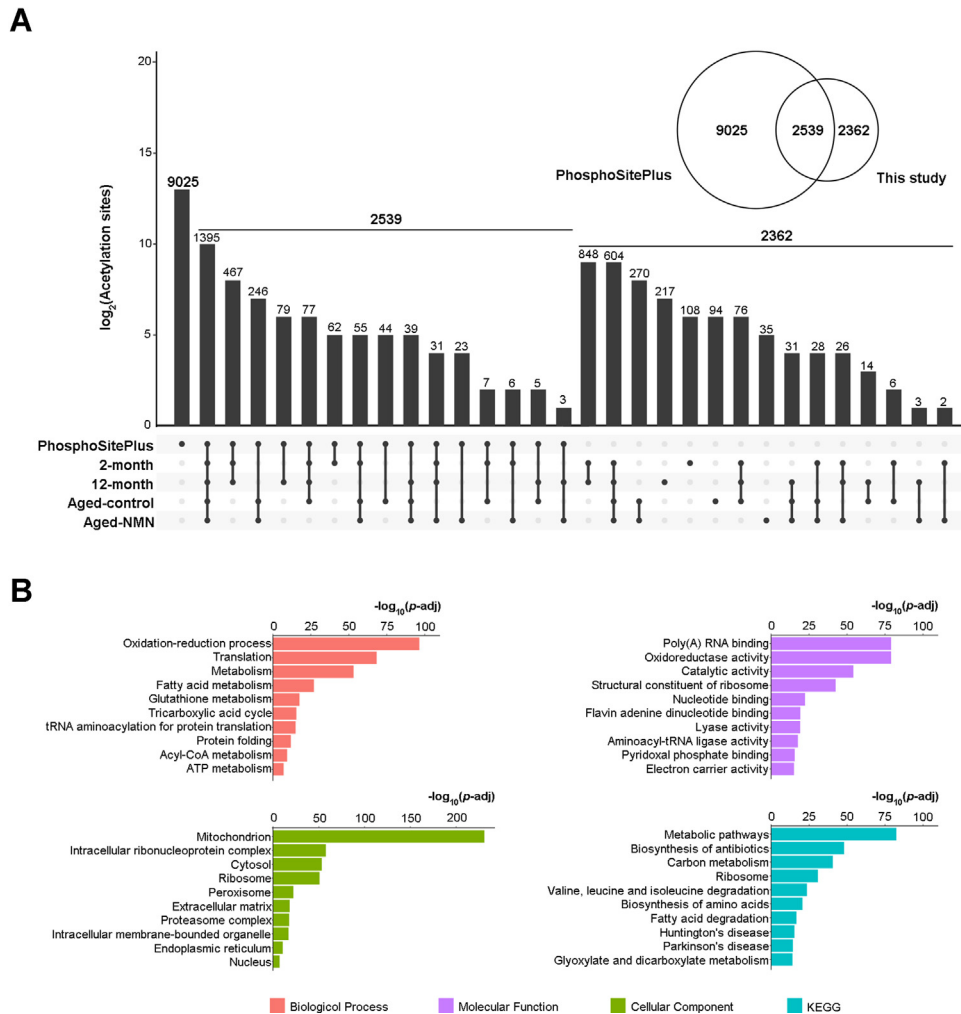


FIG. 2. **Acetylome studies reveal previously uncharacterized protein acetylation in mouse livers.** A, UpSet plot and Venn diagram showing common and specific acetylation sites between PhosphoSitePlus and the current study. B, GO analysis reveals biological process, molecular function, cellular component, and KEGG pathway of acetylated proteins in mouse livers.

increased acetylation with age (Fig. 3D and supplemental Table S3).

We calculated the sum acetylation levels of all identified sites on each protein and counted the numbers of dramatically changed acetylation sites on each protein ($p < 0.05$) (Fig. 4A and supplemental Table S4). From a total number of 1200 proteins identified from 2-month-old and 12-month-old mouse livers, acetylation in 550 proteins remained roughly unaltered. Interestingly, 75 proteins had multiple acetylation events conferring discordant dynamics with age, with some being increased while others being decreased (e.g., Protein disulfide-isomerase A3) (Fig. 4B and supplemental Table S4); 204 proteins had uniformly decreased acetylation sites (e.g., Methanethiol oxidase and 14-3-3 protein zeta/delta) (Fig. 4C and supplemental Table S4), and acetylation in 371 proteins became significantly increased in aged animals (e.g., Mitochondrial serine-pyruvate aminotransferase and Histone H2A.V) (Fig. 4D and supplemental Table S4).

Protein Acetylation as New Age-Associated Biomarkers

To explore protein acetylation as biomarkers, we designed a scheme to filter acetylation sites based on specificity with age, high reproducibility, low variation among repeats, and high intensity (Fig. 5A). High reproducibility was defined by acetylation signals detected from all four replicates for each age group. Low variation was defined by acetylation signals with coefficient of variation below 35% among replicates. High intensity referred to the average acetylation levels higher than 5×10^7 . This scheme led to us to identify two young-specific (2-months) acetylation sites (Protein FAM98B at K245 and Mitochondrial-processing peptidase subunit alpha at K477) and one age-associated (12-months) acetylation sites (Cytochrome P450 4A14 at K153) (Fig. 5, A and B). Protein FAM98B at K245 and Mitochondrial-processing peptidase subunit alpha at K477 were highly acetylated in 2-month-old mouse livers but were barely detectable at 12 months of age (Fig. 5C).

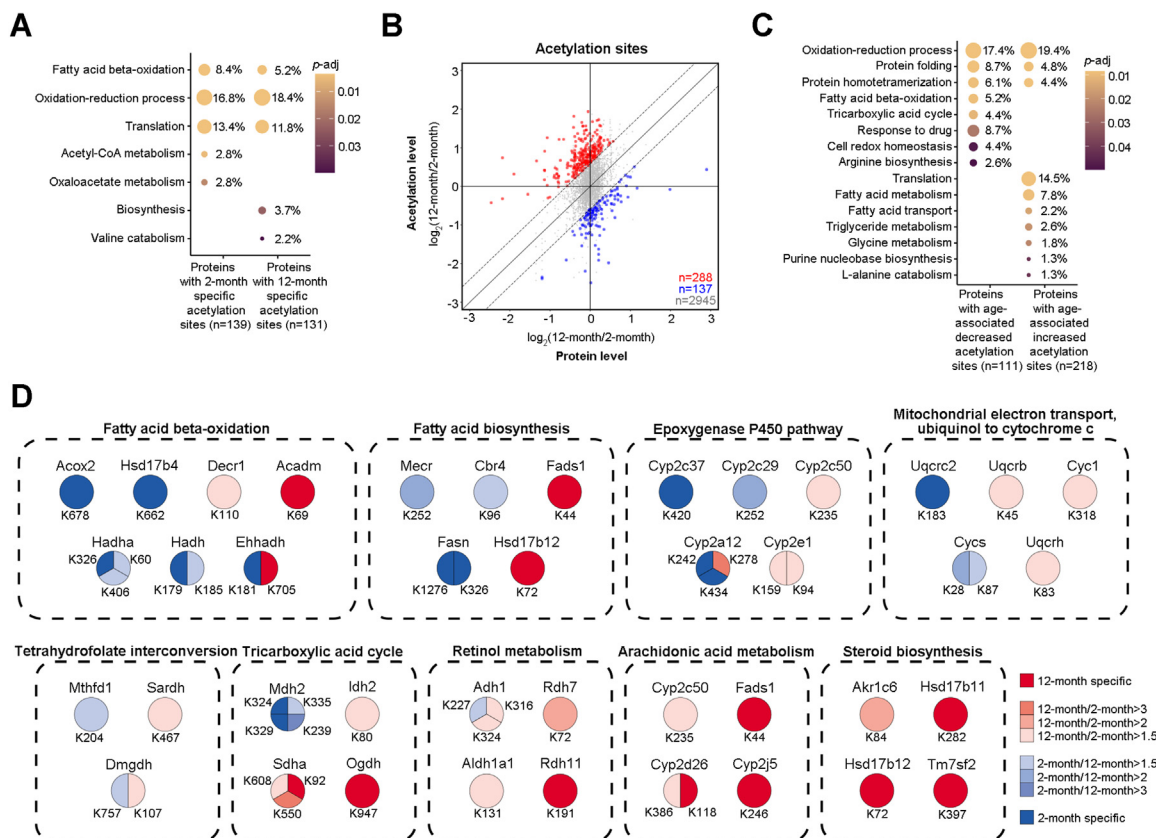


FIG. 3. Age-associated dynamics in acetylation sites. A, age-specific acetylated proteins function in diverse biological processes. B, scatterplot showing the log₂ fold change of 12 months/2 months in acetylation levels as compared to the corresponding protein levels. Each dot on the plot represents a single acetylation site. Dash lines indicate the fold change cutoff being 1.5. Red dots: age-associated increased sites (12 months/2 months>1.5, $p < 0.05$, two-tailed Student's t test); blue dots: age-associated decreased sites (2 months/12 months>1.5, $p < 0.05$, two-tailed Student's t test); gray dots: sites with no significant changes. C, function of proteins with age-associated decreased or increased acetylation in diverse biological processes. D, characterization of acetylated proteins in the oxidation–reduction process with age.

On the contrary, the acetylation of Cytochrome P450 4A14 at K153 was not identified in 2-month-old animals but was found highly modified in aged mouse livers (Fig. 5C). Sequence alignment analysis revealed that these lysine sites were evolutionarily conservative between mouse and human, suggesting their potential as aging biomarkers in mammals (Fig. 5D).

Impact of NMN Treatment on Protein Acetylation

We characterized the effect of NMN supplement on the acetylome of aged animals. Changes in acetylation were also normalized to the host protein. One hundred fifteen acetylation sites from 103 proteins were specifically identified in Aged-control mouse livers (supplemental Fig. S2B and supplemental Table S5). GO analysis showed that they were enriched in oxidation–reduction process, tricarboxylic acid cycle, citrate metabolism, and glutathione metabolism (Fig. 6A and supplemental Table S5). Only 46 acetylation sites from 44 proteins were uniquely identified in the Aged-NMN group (supplemental Fig. S2B and supplemental Table S5), with their

roles in the oxidation–reduction process (Fig. 6A and supplemental Table S5). Among 2585 acetylation sites identified in both Aged-control and Aged-NMN animals (supplemental Fig. S2B and supplemental Table S5), 108 sites from 79 proteins were significantly decreased upon the treatment of NMN (Aged-control/Aged-NMN>1.5 and $p < 0.05$) (Fig. 6B and supplemental Table S5); these proteins were enriched in oxidation–reduction process, fatty acid biosynthesis, protein homotetramerization, acyl-CoA metabolism, acetyl-CoA metabolism, and fatty acid beta-oxidation (Fig. 6C and supplemental Table S5). On the other hand, 75 sites from 52 proteins had increased acetylation (Aged-NMN/Aged-control>1.5 and $p < 0.05$) (Fig. 6B and supplemental Table S5), with their roles being enriched in oxidation–reduction process and fatty acid beta-oxidation (Fig. 6C and supplemental Table S5).

Since NMN supplementation has been shown to benefit health span (17, 20–24), we further investigated the impact of NMN on protein acetylation that normally changed during aging. Seventy-one acetylation sites in 60 proteins that

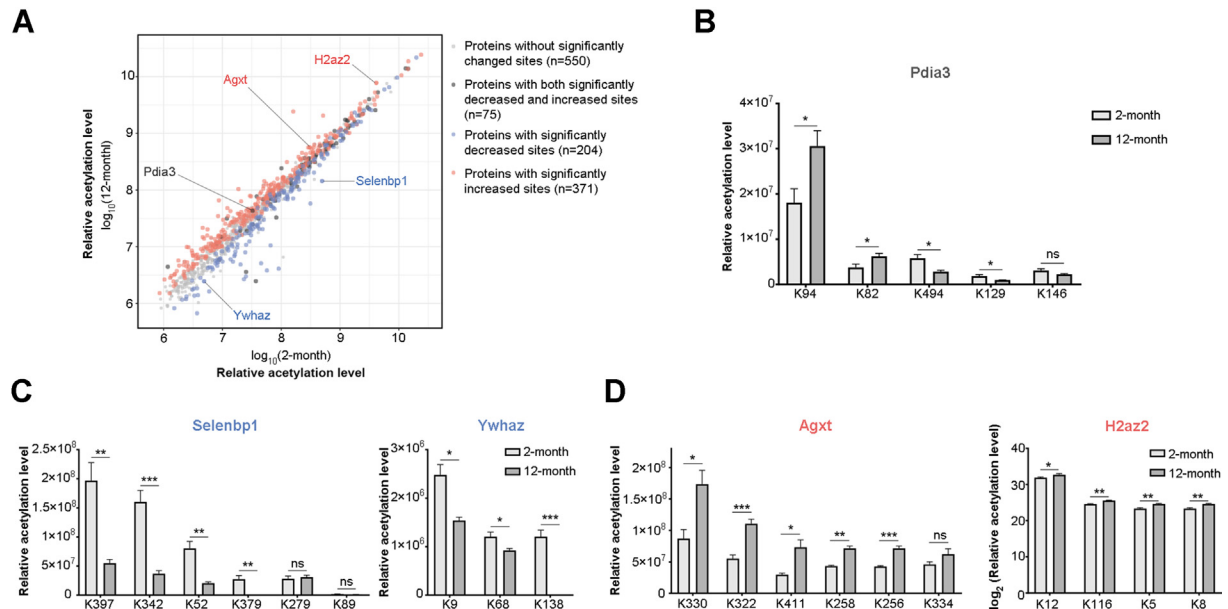


FIG. 4. Age-associated dynamics in acetylated proteins. *A*, scatterplot showing distribution of the sum acetylation levels of all identified sites on individual proteins (12 months vs. 2 months). Each dot represents a single acetylated protein. *Light gray dots*: proteins without significantly changed sites; *dark gray dots*: proteins with both significantly decreased and increased sites ($p < 0.05$ by two-tailed Student's *t* test); *blue dots*: proteins with significantly decreased acetylation sites ($p < 0.05$, two-tailed Student's *t* test); *red dots*: proteins with significantly increased acetylation sites ($p < 0.05$, two-tailed Student's *t* test). *B*, bar plots showing relative acetylation levels of representative protein with discordant dynamics. *C*, bar plots showing proteins with uniformly decreased acetylation sites. *D*, bar plots showing proteins with consistently increased acetylation sites with age (two-tailed Student's *t* test: *** $p < 0.001$; ** $p < 0.01$; * $p < 0.05$; ns, not significant).

naturally decreased with age were now reversed by NMN treatment (Fig. 6D and supplemental Table S5). GO analysis revealed their roles in oxidation–reduction process, metabolism, cell redox homeostasis, tricarboxylic acid cycle, and protein folding (Figs. 6E, S3A and supplemental Table S5). One hundred thirty-six acetylation sites in 111 proteins that

had age-modulated increase became decreased with NMN (Fig. 6D and supplemental Table S5), which were mainly involved in oxidation–reduction process, metabolic processes of fatty acid and triglyceride, translation, protein homotrimerization, response to drug, and response to cadmium ion (Figs. 6E, S3A and supplemental Table S5). In addition,

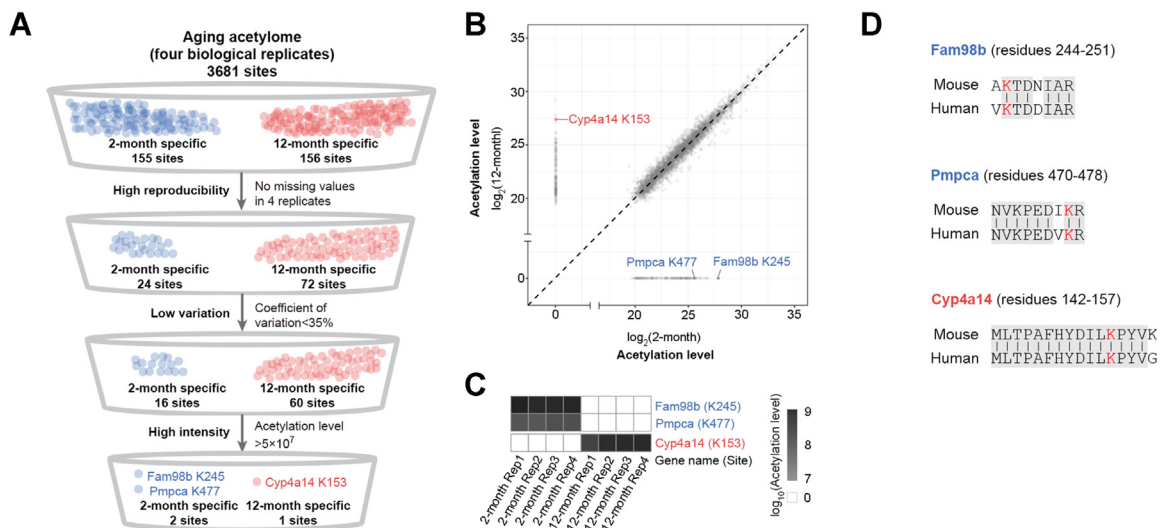


FIG. 5. Protein acetylation as new age-associated biomarkers. *A*, scheme for filtering age-associated biomarkers. *B*, scatterplot showing the log₂ intensity of acetylation levels in 12 months as compared to 2 months. Each dot represents a single acetylation site. *Blue dots*: biomarkers for young mouse livers; *red dot*: biomarker for aged mouse livers. *C*, heat map showing the acetylation levels of age-associated biomarkers. *D*, sequence alignment analysis reveals the evolutionary conservation of biomarkers between mouse and human.

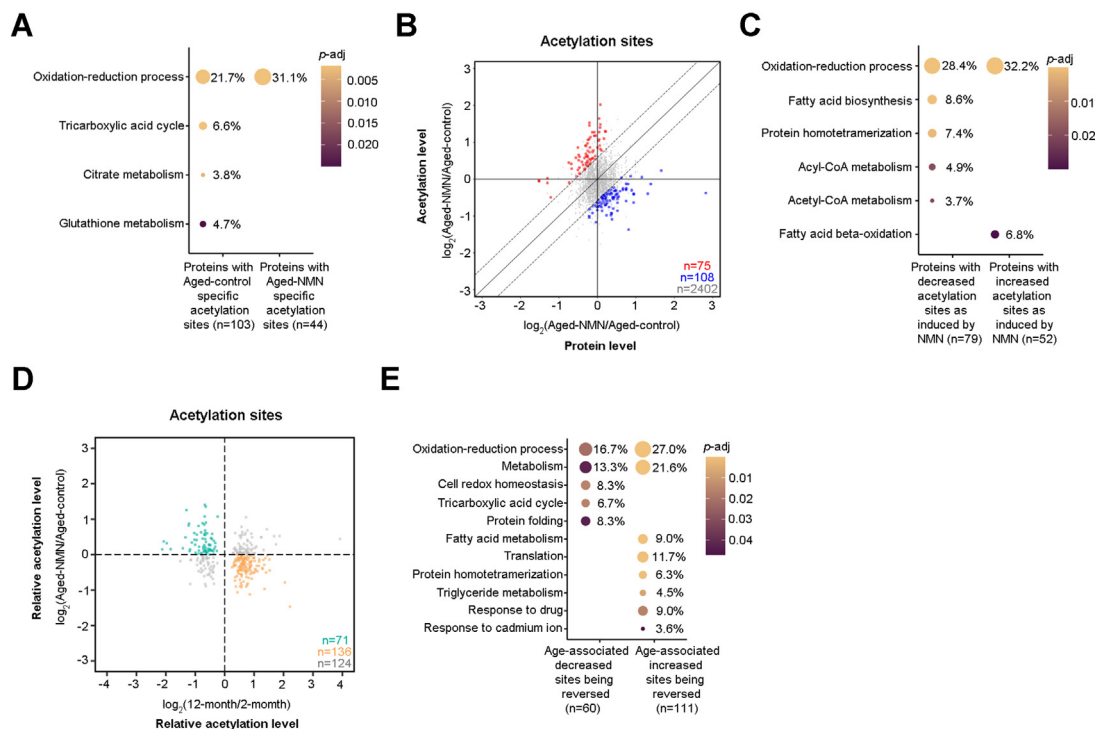


FIG. 6. Impact of NMN treatment on protein acetylation. *A*, NMN-induced acetylated proteins function in diverse biological processes. *B*, scatterplot showing the log₂ fold change of Aged-NMN/Aged-control in acetylation levels as compared to their host protein levels. Each dot represents a single acetylation site. *Dash lines* indicate the fold change cutoff being 1.5. *Red dots*: NMN-induced increased sites (Aged-NMN/Aged-control > 1.5, $p < 0.05$, two-tailed Student's t test); *blue dots*: NMN-induced decreased sites (Aged-control/Aged-NMN > 1.5, $p < 0.05$, two-tailed Student's t test); *gray dots*: sites with no significant changes. *C*, function of proteins with decreased or increased acetylation as induced by NMN in diverse biological processes. *D*, scatterplot showing age-associated decreased sites ($p < 0.05$, two-tailed Student's t test) being reversed by NMN (*green dots*) and age-associated increased sites ($p < 0.05$, two-tailed Student's t test) being reversed by NMN (*yellow dots*). *E*, NMN-reversed acetylated proteins function in diverse biological processes.

17 2-month-specific acetylation sites and 17 12-month-specific acetylation sites were reversed by NMN (supplemental Fig. S3B and supplemental Table S5). We showed the evidence that 3 acetylation sites that were highly enriched in young animals now became abundant in NMN-treated mouse livers compared to age-matched controls (supplemental Fig. S3B and supplemental Table S5). In addition, 14 acetylation sites found to be high in aged animals were significantly decreased in NMN-treated mouse livers (supplemental Fig. S3B and supplemental Table S5). Notably, the acetylation level of the aging biomarker Cytochrome P450 4A14 at K153 (see Fig. 5C) was downregulated upon NMN treatment compared to the age-matched controls (supplemental Fig. S3B). The acetylation of Protein FAM98B at K245 and Mitochondrial-processing peptidase subunit alpha at K477 as young biomarkers were not detectable in NMN-treated animals (12 months).

NMN Treatment Mildly Affects Sirtuin-Mediated Protein de-Acetylation

It has been suggested that NMN supplementation, coupled with an increased NAD⁺ level (Fig. 7A), benefits adult fitness at least in part by promoting the activity of Sirtuins, a family of

NAD-consuming deacetylases (20–22, 26–28). In our Aged-control and Aged-NMN dataset, we collectively identified 250 acetylation sites previously reported as substrates of Sirtuins (34–63) (supplemental Table S6). Surprisingly, overall levels of the acetylation sites remained roughly unchanged upon the treatment of NMN compared to those of age-matched controls (Fig. 7B and supplemental Table S6). We only observed 42 out of 250 acetylation sites altered by NMN supplementation, with 15 sites displaying decreased modification, while 27 sites being increased (Fig. 7C and supplemental Table S6). Changes in acetylation may impact protein function, yet there have been functional studies for 3 out of 42 acetylation sites being affected. Specifically, Histone H3.1 at K19 (H3K18Ac after N-terminal methionine excision co-translationally by the enzyme Methionine aminopeptidase 2) (64) had decreased acetylation upon NMN treatment (Fig. 7C), while acetylation on Histone H3.1 at K57 (H3K56Ac), with a role in transcriptional activation (65), was increased (Fig. 7C). NMN treatment also increased the acetylation of Sirt3 substrate Superoxide dismutase [Mn], mitochondrial at K122 (Fig. 7C), which has been reported to decrease the enzymatic activity as destroying superoxide anion radicals produced within the cells (66).

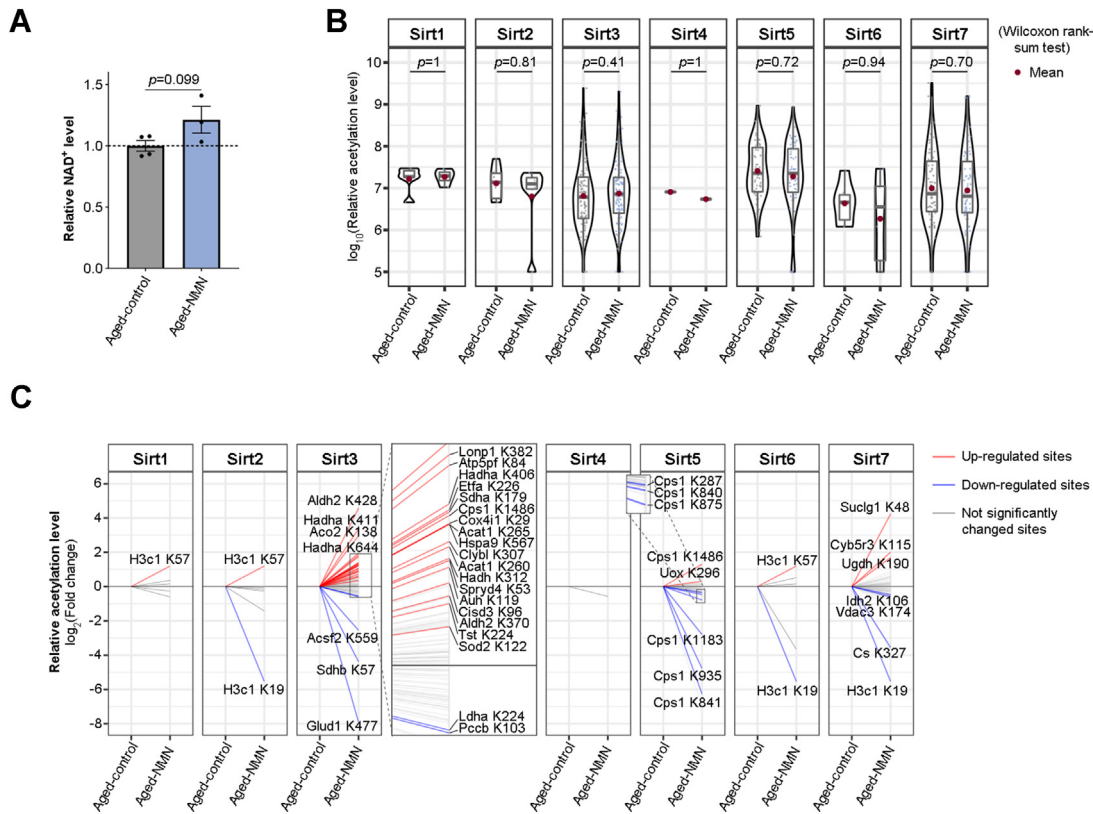


FIG. 7. NMN treatment mildly affects Sirtuin-mediated protein deacetylation. A, NMN supplementation causes an increase in NAD⁺ level. B, violin plot showing global dynamics of the acetylation levels of Sirtuin substrates by NMN treatment (Wilcoxon rank-sum test). C, line chart showing the dynamics of the acetylation levels of Sirtuin substrates by NMN treatment. Red lines: NMN-induced upregulated sites ($p < 0.05$ by two-tailed Student's *t* test); blue lines: NMN-induced downregulated sites ($p < 0.05$ by two-tailed Student's *t* test); gray lines: not significantly changed sites.

DISCUSSION

Aging is characterized by a progressive decline in cellular and organismal function that leads to reduction of fitness and increased risks to diseases and death. Aging is a complex process that can be regulated by a network of multiple mechanisms. Previous studies have focused on age-related changes on transcriptomics (67, 68), epigenetics (69), proteomics (70), and metabolomics (71), while research on protein PTM, such as acetylation, remains elusive. To investigate the dynamics of acetylation with age and upon the treatment of NMN, a precursor of health-promoting metabolite NAD⁺, we performed dual-antibody enrichment experiments combined with high-resolution LC-MS/MS analysis in mouse livers. To our knowledge, our study provides the first comprehensive and dynamic atlas of acetylome in natural aging and upon treatment of NAD⁺ booster from adult mouse tissues.

Protein lysine acetylation has been linked with cellular functions including cell cycle (72), DNA damage repair (73), autophagy (74), and diseases such as diabetes (75) and cancer (76). Our quantitative assessment reveals new features of aging acetylome from mouse livers. First, we identify 4901 acetylation sites in mouse livers, with 48.19% (2362) being

previously unknown acetylation sites in PhosphoSitePlus. Second, 7.93% sites (292 out of 3681) are decreased with age, while 12.06% sites (444 out of 3681) show increased acetylation in aged animals. We observe more acetylation sites in aged mice than in young animals. Third, proteins with a similar function may have differential acetylation with age. For example, within the biological process of oxidation-reduction, Fatty acid synthase at K326 and K1276 show decreased acetylation, while Cytochrome P450 2E1 at K94 and K159 are increased with age. Fourth, 58.83% proteins (706 out of 1200) bear more than one acetylation modification. Interestingly, 6.25% of proteins (75 out of 1200) have multiple acetylation events conferring discordant direction of change during aging. For example, the acetylation of Peroxisomal bifunctional enzyme at K181 displays a decrease, while K705 has an increase with age. Individual proteins might be substrates of different lysine acetyltransferases and/or lysine deacetylases. For example, Histone H3 is acetylated by Gcn5 and PCAF at K9 (77) and acetylated by p300/CBP at K18, K27 (78), and K56 (79). Similarly, single-lysine sites could be modulated by different enzymes, e.g., Histone H3 at K56 is deacetylated by Sirt1, Sirt2, and Sirt6 (79–81). This might partially explain why

some proteins harbor both increased and decreased acetylation sites. However, how multiple acetylation sites coordinate to affect protein function has not been studied. Our datasets provide candidates for the exploration of joint outcome by multisite acetylation on individual proteins.

During aging, acetylation on proteins in the oxidation–reduction process showed complex changes (see Fig. 3D). The oxidation–reduction process (GO: 0055114) is a metabolic process that mediates the removal or addition of one or more electrons to or from a substance, with or without the concomitant removal or addition of a proton or protons. Altered cellular redox homeostasis has been implicated as an important factor in regulating cell growth, senescence, and aging (82). The liver is a critical tissue for numerous metabolic processes including digestive absorption and uptake, synthesis, packaging, and secretion of lipids and lipoproteins (83). Here, we observed dynamic acetylation on proteins involved in fatty acid metabolism (including increased and decreased acetylation in fatty acid beta-oxidation and increased acetylation in fatty acid transport) and increased acetylation on proteins in triglyceride metabolism in aging mouse livers. The liver is also important for protein and amino acid metabolism as it is responsible for most proteins secreted into the blood (83). We found that proteins in valine catabolism, glycine metabolism, and L-alanine catabolism showed increased acetylation, which may potentially underlie functional changes in liver tissues that occur during aging.

It is interesting to note that Peleg *et al.* (9) have performed acetylomic study in *Drosophila*, revealing an increase in 79 and a decrease in 3 acetylation sites in midlife flies compared to young flies. We have performed comparative analysis between their and our datasets. ADP/ATP translocase (sesB) at K107 shows an increase in *Drosophila* head during aging, and its mouse ortholog ADP/ATP translocase 1 (Slc25a4) at K92 also increases in old mouse livers. The acetylation levels of *Drosophila* Aspartate aminotransferase (Got2) at K310 and mouse Aspartate aminotransferase, mitochondrial (Got2) at K309 both increase during aging. This evidence highlights conserved acetylation events that occur with age.

Protein acetylation may be used as aging biomarkers. It has been shown that the acetylation of K280 on Tau is linked with normal brain aging as well as a wide spectrum of human neurodegenerative diseases (13, 14). Here, we extend the scope by exploring aging acetylome, revealing new protein acetylation sites as age-related biomarkers. Specifically, we demonstrate the acetylation of Protein FAM98B at K245 and Mitochondrial-processing peptidase subunit alpha at K477 as biomarkers for young mouse livers and Cytochrome P450 4A14 at K153 as biomarker for aged animals.

The hub metabolite, NAD⁺, influences cellular physiology through multiple dimensions. Studies have shown that NAD⁺ modulates the cellular redox status (16), modifies mRNA by capping the transcript at the 5'-end (84), and rewires the acetylome by activating deacetylases, Sirtuins (20–22, 26–28).

However, the extent by which NAD⁺-induced changes in protein acetylation remains unknown. By assessing protein acetylation that normally changes with age, we note that 60.14% acetylation sites (258 out of 429) can be reversed by NMN treatment, including Cytochrome P450 4A14 at K153, the aging biomarker for aged mouse livers, suggesting that the life-beneficial effect of NMN can be at least partially reflected by changes in age-related protein acetylation. We further provide the evidence to show that NMN elicits a decrease in acetylation sites. It is still unknown whether such a decrease is due to Sirtuin-mediated deacetylation. In our dataset, however, majority of acetylation sites previously reported as substrates of Sirtuins show mild or even no change, with only 6% acetylation sites (15 out of 250 reported substrates of Sirtuins) being decreased by NMN supplementation. Though it remains to be determined, it is possible that unknown target sites may be responsive to NAD⁺-activated Sirtuins. Alternatively, nicotinamide (NAM), a metabolite converted from NAD⁺ during Sirtuin-mediated deacetylation (85), has been shown to inhibit the enzymatic activity of Sirtuins (86, 87). As a consequence, despite the fact that NAD⁺ activates Sirtuins, accumulation of NAM leads to the inhibition of Sirtuins, resulting in a perplexed outcome in protein deacetylation status. We also notice that Sirt3 appears to have primarily upregulated sites while Sirt5 has downregulated sites upon the treatment of NMN (see Fig. 7C). Sirt3 as well as Sirt5 are mainly localized in the mitochondrial matrix (81, 88), competing with the same NAD⁺ pool. Previous studies have indicated that NAD⁺ consuming Michaelis constant (Km) value for Sirt5 (ranging from 26 μM (89) to 200 μM (90)) is lower than that of Sirt3 (ranging from 280 μM (91) to 880 μM (92)). It is tempting to speculate that Sirt5 can be activated prior to Sirt3. Activation of Sirt5 results in a rapid depletion of NAD⁺ and an accumulation of NAM (86, 87), which, in turn, leads to inhibition of Sirt3-mediated deacetylation.

In summary, our study provides an important resource on protein lysine acetylation that occurs with age, laying critical foundation for the functional study of protein PTM essential for healthy aging and perhaps disease conditions.

DATA AVAILABILITY

The MS data have been deposited under the accession number IPX0004109000 at iProX (93) with the dataset identifier PXD031851. (<https://www.iprox.cn/page/project.html?id=IPX0004109000>)

Supplemental data—This article contains [supplemental data](#) (34–63).

Funding and additional information—This work was supported by grants from the National Natural Science Foundation of China to Y. Z. (32071245), the Natural Science Foundation of Shanghai to Y. Z. (20ZR1474400), and the

Shanghai Municipal Science and Technology Major Project (2019SHZDZX02) to Y. Z. and N. L.

Author contributions—J. L. and N. L. contributed to concept and design of the study. J. L., Y. C. and Y. Z. contributed to the detection of acetylome. K. N., J. Q., Y. L., and Z. Z. contributed to the detection of NAD⁺. J. L., K. N., H. W., and Y. Y. collected the mouse samples. J. L. and D. L. performed the statistical analysis. J. L. and N. L. wrote the manuscript.

Conflict of interest—The authors declare that they have no conflicts of interest with the contents of this article.

Abbreviations—The abbreviations used are: Ac, acetylation; ACN, acetonitrile; DAVID, Database for Annotation, Visualization and Integrated Discovery; EDTA, ethylenediaminetetraacetic acid; FA, formic acid; GO, Gene Ontology; K, lysine; KEGG, Kyoto Encyclopedia of Genes and Genomes; LC-MS/MS, liquid chromatography with tandem mass spectrometry; MeOH, methanol; NAD⁺, nicotinamide adenine dinucleotide; NAM, nicotinamide; NaCl, sodium chloride; NH₄OH, ammonium hydroxide; NH₄OAc, ammonium acetate; NMN, beta-nicotinamide mononucleotide; PTM, post-translational modification; Tau, Microtubule-associated protein tau; TFA, trifluoroacetic acid; Tris-HCl, Tris-hydrochloride.

Received February 15, 2022, and in revised from, June 25, 2022
Published, MCPRO Papers in Press, August 3, 2022, <https://doi.org/10.1016/j.mcpro.2022.100276>

REFERENCES

- Eberharter, A., and Becker, P. B. (2002) Histone acetylation: a switch between repressive and permissive chromatin. Second in review series on chromatin dynamics. *EMBO Rep.* **3**, 224–229
- Schwer, B., Bunkenborg, J., Verdin, R. O., Andersen, J. S., and Verdin, E. (2006) Reversible lysine acetylation controls the activity of the mitochondrial enzyme acetyl-CoA synthetase 2. *Proc. Natl. Acad. Sci. U. S. A.* **103**, 10224–10229
- Cohen, T. J., Hwang, A. W., Restrepo, C. R., Yuan, C. X., Trojanowski, J. Q., and Lee, V. M. (2015) An acetylation switch controls TDP-43 function and aggregation propensity. *Nat. Commun.* **6**, 5845
- Zhao, S., Xu, W., Jiang, W., Yu, W., Lin, Y., Zhang, T., et al. (2010) Regulation of cellular metabolism by protein lysine acetylation. *Science* **327**, 1000–1004
- Ree, R., Varland, S., and Arnesen, T. (2018) Spotlight on protein N-terminal acetylation. *Exp. Mol. Med.* **50**, 1–13
- Rahman, M., Nirala, N. K., Singh, A., Zhu, L. J., Taguchi, K., Bamba, T., et al. (2014) Drosophila Sirt2/mammalian SIRT3 deacetylates ATP synthase β and regulates complex V activity. *J. Cell Biol.* **206**, 289–305
- Weinert, B. T., Narita, T., Satpathy, S., Srinivasan, B., Hansen, B. K., Schölz, C., et al. (2018) Time-resolved analysis reveals rapid dynamics and broad scope of the CBF/p300 acetylome. *Cell* **174**, 231–244.e212
- Choudhary, C., Kumar, C., Gnad, F., Nielsen, M. L., Rehman, M., Walther, T. C., et al. (2009) Lysine acetylation targets protein complexes and co-regulates major cellular functions. *Science* **325**, 834–840
- Peleg, S., Feller, C., Fome, I., Schiller, E., Sévin, D. C., Schauer, T., et al. (2016) Life span extension by targeting a link between metabolism and histone acetylation in Drosophila. *EMBO Rep.* **17**, 455–469
- Hebert, A. S., Dittenhafer-Reed, K. E., Yu, W., Bailey, D. J., Selen, E. S., Boersma, M. D., et al. (2013) Calorie restriction and SIRT3 trigger global reprogramming of the mitochondrial protein acetylome. *Mol. Cell* **49**, 186–199
- Lundby, A., Lage, K., Weinert, B. T., Bekker-Jensen, D. B., Secher, A., Skovgaard, T., et al. (2012) Proteomic analysis of lysine acetylation sites in rat tissues reveals organ specificity and subcellular patterns. *Cell Rep.* **2**, 419–431
- López-Otín, C., Blasco, M. A., Partridge, L., Serrano, M., and Kroemer, G. (2013) The hallmarks of aging. *Cell* **153**, 1194–1217
- Cohen, T. J., Guo, J. L., Hurtado, D. E., Kwong, L. K., Mills, I. P., Trojanowski, J. Q., et al. (2011) The acetylation of tau inhibits its function and promotes pathological tau aggregation. *Nat. Commun.* **2**, 252
- Irwin, D. J., Cohen, T. J., Grossman, M., Arnold, S. E., Xie, S. X., Lee, V. M., et al. (2012) Acetylated tau, a novel pathological signature in Alzheimer's disease and other tauopathies. *Brain* **135**, 807–818
- Yeo, D., Kang, C., and Ji, L. L. (2020) Aging alters acetylation status in skeletal and cardiac muscles. *Geroscience* **42**, 963–976
- Katsyuba, E., Romani, M., Hofer, D., and Auwerx, J. (2020) NAD(+) homeostasis in health and disease. *Nat. Metab.* **2**, 9–31
- Yoshino, J., Mills, K. F., Yoon, M. J., and Imai, S. (2011) Nicotinamide mononucleotide, a key NAD(+) intermediate, treats the pathophysiology of diet- and age-induced diabetes in mice. *Cell Metab.* **14**, 528–536
- Massudi, H., Grant, R., Braid, N., Guest, J., Farnsworth, B., and Guillemain, G. J. (2012) Age-associated changes in oxidative stress and NAD+ metabolism in human tissue. *PLoS One* **7**, e42357
- Zhu, X. H., Lu, M., Lee, B. Y., Ugurbil, K., and Chen, W. (2015) *In vivo* NAD assay reveals the intracellular NAD contents and redox state in healthy human brain and their age dependences. *Proc. Natl. Acad. Sci. U. S. A.* **112**, 2876–2881
- Anderson, R. M., Bitterman, K. J., Wood, J. G., Medvedik, O., Cohen, H., Lin, S. S., et al. (2002) Manipulation of a nuclear NAD+ salvage pathway delays aging without altering steady-state NAD+ levels. *J. Biol. Chem.* **277**, 18881–18890
- Mouchiroud, L., Houtkooper, R. H., Moullan, N., Katsyuba, E., Ryu, D., Cantó, C., et al. (2013) The NAD(+)/Sirtuin pathway modulates longevity through activation of mitochondrial UPR and FOXO signaling. *Cell* **154**, 430–441
- Balan, V., Miller, G. S., Kaplun, L., Balan, K., Chong, Z. Z., Li, F., et al. (2008) Life span extension and neuronal cell protection by Drosophila nicotinamidase. *J. Biol. Chem.* **283**, 27810–27819
- Zhang, H., Ryu, D., Wu, Y., Gariani, K., Wang, X., Luan, P., et al. (2016) NAD+ repletion improves mitochondrial and stem cell function and enhances life span in mice. *Science* **352**, 1436–1443
- Amano, H., Chaudhury, A., Rodriguez-Aguayo, C., Lu, L., Akhanov, V., Catic, A., et al. (2019) Telomere dysfunction induces sirtuin repression that drives telomere-dependent disease. *Cell Metab.* **29**, 1274–1290.e1279
- Rajman, L., Chwalek, K., and Sinclair, D. A. (2018) Therapeutic potential of NAD-boosting molecules: the *in vivo* evidence. *Cell Metab.* **27**, 529–547
- Scheibye-Knudsen, M., Mitchell, S. J., Fang, E. F., Iyama, T., Ward, T., Wang, J., et al. (2014) A high-fat diet and NAD(+) activate Sirt1 to rescue premature aging in cockayne syndrome. *Cell Metab.* **20**, 840–855
- Cantó, C., Houtkooper, R. H., Pirinen, E., Youn, D. Y., Oosterveer, M. H., Cen, Y., et al. (2012) The NAD(+) precursor nicotinamide riboside enhances oxidative metabolism and protects against high-fat diet-induced obesity. *Cell Metab.* **15**, 838–847
- Brown, K. D., Maqsood, S., Huang, J. Y., Pan, Y., Harkcom, W., Li, W., et al. (2014) Activation of SIRT3 by the NAD+ precursor nicotinamide riboside protects from noise-induced hearing loss. *Cell Metab.* **20**, 1059–1068
- Imai, S., Armstrong, C. M., Kaerberlein, M., and Guarente, L. (2000) Transcriptional silencing and longevity protein Sir2 is an NAD-dependent histone deacetylase. *Nature* **403**, 795–800
- Tyanova, S., Temu, T., and Cox, J. (2016) The MaxQuant computational platform for mass spectrometry-based shotgun proteomics. *Nat. Protoc.* **11**, 2301–2319
- Huang da, W., Sherman, B. T., and Lempicki, R. A. (2009) Systematic and integrative analysis of large gene lists using DAVID bioinformatics resources. *Nat. Protoc.* **4**, 44–57
- Huang da, W., Sherman, B. T., and Lempicki, R. A. (2009) Bioinformatics enrichment tools: paths toward the comprehensive functional analysis of large gene lists. *Nucl. Acids Res.* **37**, 1–13
- Hornbeck, P. V., Zhang, B., Murray, B., Kornhauser, J. M., Latham, V., and Skrzypek, E. (2015) PhosphoSitePlus, 2014: mutations, PTMs and recalibrations. *Nucl. Acids Res.* **43**, D512–D520

34. Bheda, P., Jing, H., Wolberger, C., and Lin, H. (2016) The substrate specificity of sirtuins. *Annu. Rev. Biochem.* **85**, 405–429
35. Chen, Y., Zhao, W., Yang, J. S., Cheng, Z., Luo, H., Lu, Z., et al. (2012) Quantitative acetylome analysis reveals the roles of SIRT1 in regulating diverse substrates and cellular pathways. *Mol. Cell Proteomics* **11**, 1048–1062
36. Drazic, A., Myklebust, L. M., Ree, R., and Arnesen, T. (2016) The world of protein acetylation. *Biochim. Biophys. Acta* **1864**, 1372–1401
37. Rardin, M. J., Newman, J. C., Held, J. M., Cusack, M. P., Sorensen, D. J., Li, B., et al. (2013) Label-free quantitative proteomics of the lysine acetylome in mitochondria identifies substrates of SIRT3 in metabolic pathways. *Proc. Natl. Acad. Sci. U. S. A.* **110**, 6601–6606
38. Laurent, G., German, N. J., Saha, A. K., de Boer, V. C., Davies, M., Koves, T. R., et al. (2013) SIRT4 coordinates the balance between lipid synthesis and catabolism by repressing malonyl CoA decarboxylase. *Mol. Cell* **50**, 686–698
39. Nakagawa, T., Lomb, D. J., Haigis, M. C., and Guarente, L. (2009) SIRT5 Deacetylates carbamoyl phosphate synthetase 1 and regulates the urea cycle. *Cell* **137**, 560–570
40. Xu, Y. S., Liang, J. J., Wang, Y., Zhao, X. J., Xu, L., Xu, Y. Y., et al. (2016) STAT3 undergoes acetylation-dependent mitochondrial translocation to regulate pyruvate metabolism. *Sci. Rep.* **6**, 39517
41. Nakamura, Y., Ogura, M., Ogura, K., Tanaka, D., and Inagaki, N. (2012) SIRT5 deacetylates and activates urate oxidase in liver mitochondria of mice. *FEBS Lett.* **586**, 4076–4081
42. Guan, D., Lim, J. H., Peng, L., Liu, Y., Lam, M., Seto, E., et al. (2014) Deacetylation of the tumor suppressor protein PML regulates hydrogen peroxide-induced cell death. *Cell Death Dis.* **5**, e1340
43. Schlicker, C., Gertz, M., Papatheodorou, P., Kachholz, B., Becker, C. F., and Steegborn, C. (2008) Substrates and regulation mechanisms for the human mitochondrial sirtuins Sirt3 and Sirt5. *J. Mol. Biol.* **382**, 790–801
44. Michishita, E., McCord, R. A., Berber, E., Kioi, M., Padilla-Nash, H., Damian, M., et al. (2008) SIRT6 is a histone H3 lysine 9 deacetylase that modulates telomeric chromatin. *Nature* **452**, 492–496
45. McCord, R. A., Michishita, E., Hong, T., Berber, E., Boxer, L. D., Kusumoto, R., et al. (2009) SIRT6 stabilizes DNA-dependent protein kinase at chromatin for DNA double-strand break repair. *Aging (Albany NY)* **1**, 109–121
46. Kawahara, T. L., Michishita, E., Adler, A. S., Damian, M., Berber, E., Lin, M., et al. (2009) SIRT6 links histone H3 lysine 9 deacetylation to NF- κ B-dependent gene expression and organismal life span. *Cell* **136**, 62–74
47. Sebastián, C., Zwaans, B. M., Silberman, D. M., Gymrek, M., Goren, A., Zhong, L., et al. (2012) The histone deacetylase SIRT6 is a tumor suppressor that controls cancer metabolism. *Cell* **151**, 1185–1199
48. Michishita, E., McCord, R. A., Boxer, L. D., Barber, M. F., Hong, T., Gozani, O., et al. (2009) Cell cycle-dependent deacetylation of telomeric histone H3 lysine K56 by human SIRT6. *Cell Cycle* **8**, 2664–2666
49. Yang, B., Zwaans, B. M., Eckersdorff, M., and Lombard, D. B. (2009) The sirtuin SIRT6 deacetylates H3 K56Ac *in vivo* to promote genomic stability. *Cell Cycle* **8**, 2662–2663
50. Tasselli, L., Xi, Y., Zheng, W., Tennen, R. I., Odrowaz, Z., Simeoni, F., et al. (2016) SIRT6 deacetylates H3K18ac at pericentric chromatin to prevent mitotic errors and cellular senescence. *Nat. Struct. Mol. Biol.* **23**, 434–440
51. Wang, W. W., Zeng, Y., Wu, B., Deiters, A., and Liu, W. R. (2016) A chemical biology approach to reveal Sirt6-targeted histone H3 sites in nucleosomes. *ACS Chem. Biol.* **11**, 1973–1981
52. Lee, N., Kim, D. K., Kim, E. S., Park, S. J., Kwon, J. H., Shin, J., et al. (2014) Comparative interactomes of SIRT6 and SIRT7: implication of functional links to aging. *Proteomics* **14**, 1610–1622
53. Bhardwaj, A., and Das, S. (2016) SIRT6 deacetylates PKM2 to suppress its nuclear localization and oncogenic functions. *Proc. Natl. Acad. Sci. U. S. A.* **113**, E538–E547
54. Dominy, J. E., Jr., Lee, Y., Jedrychowski, M. P., Chim, H., Jurczak, M. J., Camporez, J. P., et al. (2012) The deacetylase Sirt6 activates the acetyltransferase GCN5 and suppresses hepatic gluconeogenesis. *Mol. Cell* **48**, 900–913
55. Khongkow, M., Olmos, Y., Gong, C., Gomes, A. R., Monteiro, L. J., Yagüe, E., et al. (2013) SIRT6 modulates paclitaxel and epirubicin resistance and survival in breast cancer. *Carcinogenesis* **34**, 1476–1486
56. Barber, M. F., Michishita-Kioi, E., Xi, Y., Tasselli, L., Kioi, M., Moqtaderi, Z., et al. (2012) SIRT7 links H3K18 deacetylation to maintenance of oncogenic transformation. *Nature* **487**, 114–118
57. Chen, S., Seiler, J., Santiago-Reichert, M., Felbel, K., Grummt, I., and Voit, R. (2013) Repression of RNA polymerase I upon stress is caused by inhibition of RNA-dependent deacetylation of PAF53 by SIRT7. *Mol. Cell* **52**, 303–313
58. Chen, S., Blank, M. F., Iyer, A., Huang, B., Wang, L., Grummt, I., et al. (2016) SIRT7-dependent deacetylation of the U3-55k protein controls pre-rRNA processing. *Nat. Commun.* **7**, 10734
59. Blank, M. F., Chen, S., Poetz, F., Schnölzer, M., Voit, R., and Grummt, I. (2017) SIRT7-dependent deacetylation of CDK9 activates RNA polymerase II transcription. *Nucl. Acids Res.* **45**, 2675–2686
60. Ryu, D., Jo, Y. S., Lo Sasso, G., Stein, S., Zhang, H., Perino, A., et al. (2014) A SIRT7-dependent acetylation switch of GABP β 1 controls mitochondrial function. *Cell Metab.* **20**, 856–869
61. Karim, M. F., Yoshizawa, T., Sobuz, S. U., Sato, Y., and Yamagata, K. (2017) Sirtuin 7-dependent deacetylation of DDB1 regulates the expression of nuclear receptor TR4. *Biochem. Biophys. Res. Commun.* **490**, 423–428
62. Vakhrusheva, O., Smolka, C., Gajawada, P., Kostin, S., Boettger, T., Kubin, T., et al. (2008) Sirt7 increases stress resistance of cardiomyocytes and prevents apoptosis and inflammatory cardiomyopathy in mice. *Circ. Res.* **102**, 703–710
63. Zhang, C., Zhai, Z., Tang, M., Cheng, Z., Li, T., Wang, H., et al. (2017) Quantitative proteome-based systematic identification of SIRT7 substrates. *Proteomics*. <https://doi.org/10.1002/pmic.201600395>
64. Wang, Z., Zang, C., Rosenfeld, J. A., Schones, D. E., Barski, A., Cuddapah, S., et al. (2008) Combinatorial patterns of histone acetylations and methylations in the human genome. *Nat. Genet.* **40**, 897–903
65. Williams, S. K., Truong, D., and Tyler, J. K. (2008) Acetylation in the globular core of histone H3 on lysine-56 promotes chromatin disassembly during transcriptional activation. *Proc. Natl. Acad. Sci. U. S. A.* **105**, 9000–9005
66. Tao, R., Coleman, M. C., Pennington, J. D., Ozden, O., Park, S. H., Jiang, H., et al. (2010) Sirt3-mediated deacetylation of evolutionarily conserved lysine 122 regulates MnSOD activity in response to stress. *Mol. Cell* **40**, 893–904
67. White, R. R., Milholland, B., MacRae, S. L., Lin, M., Zheng, D., and Vijg, J. (2015) Comprehensive transcriptional landscape of aging mouse liver. *BMC Genomics* **16**, 899
68. Schaum, N., Lehallier, B., Hahn, O., Pálovics, R., Hosseinzadeh, S., Lee, S. E., et al. (2020) Ageing hallmarks exhibit organ-specific temporal signatures. *Nature* **583**, 596–602
69. Ma, Z., Wang, H., Cai, Y., Wang, H., Niu, K., Wu, X., et al. (2018) Epigenetic drift of H3K27me3 in aging links glycolysis to healthy longevity in *Drosophila*. *Elife* **7**, e35368
70. Yang, L., Ma, Z., Wang, H., Niu, K., Cao, Y., Sun, L., et al. (2019) Ubiquitylome study identifies increased histone 2A ubiquitylation as an evolutionarily conserved aging biomarker. *Nat. Commun.* **10**, 2191
71. Houtkooper, R. H., Argmann, C., Houten, S. M., Cantó, C., Jenning, E. H., Andreux, P. A., et al. (2011) The metabolic footprint of aging in mice. *Sci. Rep.* **1**, 134
72. Zhang, J., Shi, X., Li, Y., Kim, B. J., Jia, J., Huang, Z., et al. (2008) Acetylation of Smc3 by Eco1 is required for S phase sister chromatid cohesion in both human and yeast. *Mol. Cell* **31**, 143–151
73. Jacquet, K., Fradet-Turcotte, A., Avvakumov, N., Lambert, J. P., Roques, C., Pandita, R. K., et al. (2016) The TIP60 complex regulates bivalent chromatin recognition by 53BP1 through direct H4K20me binding and H2AK15 acetylation. *Mol. Cell* **62**, 409–421
74. Lin, S. Y., Li, T. Y., Liu, Q., Zhang, C., Li, X., Chen, Y., et al. (2012) GSK3-TIP60-ULK1 signaling pathway links growth factor deprivation to autophagy. *Science* **336**, 477–481
75. Iyer, A., Fairlie, D. P., and Brown, L. (2012) Lysine acetylation in obesity, diabetes and metabolic disease. *Immunol. Cell Biol.* **90**, 39–46
76. Gil, J., Ramírez-Torres, A., and Encarnación-Guevara, S. (2017) Lysine acetylation and cancer: a proteomics perspective. *J. Proteomics* **150**, 297–309
77. Gao, B., Kong, Q., Zhang, Y., Yun, C., Dent, S. Y. R., Song, J., et al. (2017) The histone acetyltransferase Gcn5 positively regulates T cell activation. *J. Immunol.* **198**, 3927–3938
78. Jin, Q., Yu, L. R., Wang, L., Zhang, Z., Kasper, L. H., Lee, J. E., et al. (2011) Distinct roles of GCN5/PCAF-mediated H3K9ac and CBP/p300-mediated H3K18/27ac in nuclear receptor transactivation. *EMBO J.* **30**, 249–262

79. Das, C., Lucia, M. S., Hansen, K. C., and Tyler, J. K. (2009) CBP/p300-mediated acetylation of histone H3 on lysine 56. *Nature* **459**, 113–117
80. Yuan, J., Pu, M., Zhang, Z., and Lou, Z. (2009) Histone H3-K56 acetylation is important for genomic stability in mammals. *Cell Cycle* **8**, 1747–1753
81. Kong, S., Kim, S. J., Sandal, B., Lee, S. M., Gao, B., Zhang, D. D., et al. (2011) The type III histone deacetylase Sirt1 protein suppresses p300-mediated histone H3 lysine 56 acetylation at Bclaf1 promoter to inhibit T cell activation. *J. Biol. Chem.* **286**, 16967–16975
82. Kwon, Y. W., Masutani, H., Nakamura, H., Ishii, Y., and Yodoi, J. (2003) Redox regulation of cell growth and cell death. *Biol. Chem.* **384**, 991–996
83. Trefts, E., Gannon, M., and Wasserman, D. H. (2017) The liver. *Curr. Biol.* **27**, R1147–R1151
84. Jiao, X., Doamekpor, S. K., Bird, J. G., Nickels, B. E., Tong, L., Hart, R. P., et al. (2017) 5' end nicotinamide adenine dinucleotide cap in human cells promotes RNA decay through DXO-mediated deNADding. *Cell* **168**, 1015–1027.e1010
85. Tanner, K. G., Landry, J., Sternglanz, R., and Denu, J. M. (2000) Silent information regulator 2 family of NAD- dependent histone/protein deacetylases generates a unique product, 1-O-acetyl-ADP-ribose. *Proc. Natl. Acad. Sci. U. S. A.* **97**, 14178–14182
86. Bitterman, K. J., Anderson, R. M., Cohen, H. Y., Latorre-Esteves, M., and Sinclair, D. A. (2002) Inhibition of silencing and accelerated aging by nicotinamide, a putative negative regulator of yeast sir2 and human SIRT1. *J. Biol. Chem.* **277**, 45099–45107
87. Landry, J., Slama, J. T., and Sternglanz, R. (2000) Role of NAD(+) in the deacetylase activity of the SIR2-like proteins. *Biochem. Biophys. Res. Commun.* **278**, 685–690
88. Schwer, B., North, B. J., Frye, R. A., Ott, M., and Verdin, E. (2002) The human silent information regulator (Sir)2 homologue hSIRT3 is a mitochondrial nicotinamide adenine dinucleotide-dependent deacetylase. *J. Cell Biol.* **158**, 647–657
89. Roessler, C., Tüting, C., Meleshin, M., Steegborn, C., and Schutkowski, M. (2015) A novel continuous assay for the deacetylase sirtuin 5 and other deacetylases. *J. Med. Chem.* **58**, 7217–7223
90. Madsen, A. S., Andersen, C., Daoud, M., Anderson, K. A., Laursen, J. S., Chakladar, S., et al. (2016) Investigating the sensitivity of NAD+-dependent sirtuin deacylation activities to NADH. *J. Biol. Chem.* **291**, 7128–7141
91. Jin, L., Galonek, H., Israelian, K., Choy, W., Morrison, M., Xia, Y., et al. (2009) Biochemical characterization, localization, and tissue distribution of the longer form of mouse SIRT3. *Protein Sci.* **18**, 514–525
92. Hirschey, M. D., Shimazu, T., Jing, E., Grueter, C. A., Collins, A. M., Auizerat, B., et al. (2011) SIRT3 deficiency and mitochondrial protein hyperacetylation accelerate the development of the metabolic syndrome. *Mol. Cell* **44**, 177–190
93. Ma, J., Chen, T., Wu, S., Yang, C., Bai, M., Shu, K., et al. (2019) iProX: an integrated proteome resource. *Nucl. Acids Res.* **47**, D1211–D1217